Feasibility Study of Energy Self-sufficiency on Chuja Island, Korea using Wind Energy

Keonwoo Lee*, Eelhwan Kim**, Kyungnam Ko*‡

*Faculty of Wind Energy Engineering, Graduate School, Jeju National University, 102 Jejudaehakno, Jeju, 63243, Rep. of Korea

**Department of Electrical Engineering, Jeju National University, 102 Jejudaehakno, Jeju, 63243, Rep. of Korea

leekw2015@jejunu.ac.kr, ehkim@jejunu.ac.kr, gnkor2@jejunu.ac.kr

‡Corresponding Author; Kyungnam Ko, Faculty of Wind Energy Engineering, Graduate School, Jeju National University, 102 Jejudaehakno, Jeju, 63243, Rep. of Korea, Tel: +82 64 754 4401, Fax: +82 64 702 2479, gnkor2@jejunu.ac.kr

Received: 23.05.2019 Accepted:20.06.2019

Abstract- A study on the possibility of energy self-sufficiency was conducted on Chuja Island, South Korea. The one-year wind data from 40 m to 80 m above ground level were collected from the Light Detection and Ranging (LiDAR) device. Fundamental characteristics of the wind data were analysed in detail. Then, the Measure-Correlate-Predict (MCP) technique was carried out to adjust the one-year wind data to long-term wind climate on the island using a nearby 25-year reanalysis wind data set. The power curves of three commercial wind turbines were applied to calculate the Annual Energy Productions (AEPs) for 25 years. Finally, an economic feasibility analysis was performed and then the possibility of energy self-sufficiency was assessed on the basis of actual electricity consumption of the island. As a result, the estimated annual Capacity Factors (CFs) were about 40 % to 50 %, which is similar to those of generic offshore wind farms. Also, the Internal Rate of Return (IRR) and Benefit-Cost Ratio (BCR) were 13.63 % and 1.77, respectively. The possibility of energy self-sufficiency on Chuja Island is revealed in this paper.

Keywords Wind energy; Wind data; Light Detection and Ranging (LiDAR) system; Economic feasibility analysis; Energy self-sufficiency.

1. Introduction

Wind energy is normally considered one of the leading renewable energies. The market of wind energy has been growing and improving. The Capital Expenditure (CapEx), Capacity Factor (CF), and Levelized Cost of Energy (LCOE) of onshore wind energy were improved to $1,477/kW, 29 %, and $0.06/kWh, respectively, on world average in 2017 [1]. Also, worldwide offshore wind power capacity has risen from 1,442 MW in 2008 to 19,275 MW in 2017, an annual growth rate of about 33 % [2].

With an increase of on and offshore wind power plants, installing many meteorological masts is inevitable prior to the construction of the plants for wind resource measurement and after the construction for power performance measurement. However, it is generally very expensive and time-consuming to install tall met masts, which is the reason a Remote Sensing Device (RSD) such as Light Detection and Ranging (LiDAR) or Sonic Detection and Ranging (SoDAR) systems has been obtaining popularity [3,4]. That is, an RSD has the advantages of being highly portable and having a wider measurement range from 30 m to 200 m above ground level (a.g.l.). An RSD can be used to test wind turbine power performance more accurately by applying a rotor equivalent wind speed in compliance with International Electrotechnical Commission (IEC) 61400-12-1 ed.2 [5]. The LiDAR system has been applied in the wind industry more than the SoDAR system since the price of the LiDAR system has been decreasing with enhancement of its performance.

There have been many studies using the LiDAR system for wind energy application. The verification of LiDAR wind data measured on simple and complex terrain was carried out by Kim et al. [6], while it was performed under offshore circumstances [7]. Furthermore, the LiDAR systems were also utilized for checking wind turbine yaw misalignment [8]. The LiDAR systems have been employed for capturing wind shear up to 300 m a.g.l. [9] and the speedup effect on a hill [10]. As LiDAR measurements have been establishing reliability, these were used for the economic feasibility study [11] as well as the analysis of wind characteristics [12].

Wind analysts may be able to use LiDAR measurements instead of met mast measurements collected on small islands for determining the possibility of energy self-sufficiency because it is generally more difficult to transport, install, operate, and maintain met masts on small islands compared with inland locations.

This study aims to analyze the feasibility of energy self-sufficiency on Chuja Island, Korea, using LiDAR measurement data. The ground-based LiDAR system was deployed at a site on the island to measure wind condition from 40 m to 80 m a.g.l. and the measurement campaign was performed for one year. After collecting and filtering the data, the wind characteristics were analyzed in detail. Then, the Measure-Correlate-Predict (MCP) method was applied with the one-year LiDAR measurements to adjust the long-term wind climate. Finally, the financial performance was estimated using three types of wind turbines operating at the site in order to determine the possibility of energy self-sufficiency.

2. Test Setup

Fig. 1 shows the location of the LiDAR device on Chuja Island, Korea. Chuja Island is situated between the southern coast of the Korean peninsula and Jeju Island. The island is surrounded by the sea and its area is 7.05 km^2. The highest altitude of the island is about 100 m above sea level and the population is about 1,800. The WindCube v2 model of the LiDAR system was installed for this study.

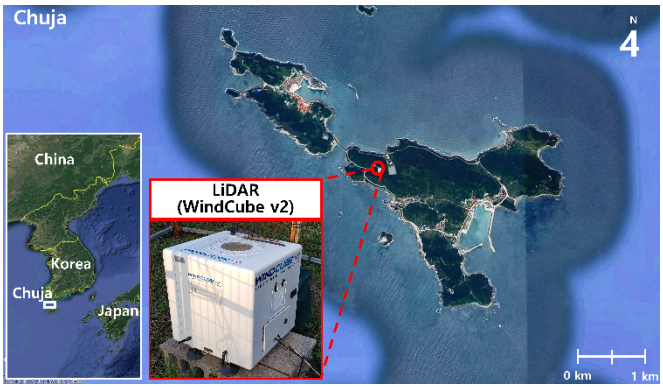

Fig. 1. Location of LiDAR device on Chuja Island, Korea.

Table 1 represents the site and measurement conditions with LiDAR specification. The roughness class around the LiDAR was 1.28, which corresponds to flat and open terrain [4]. The 10-min average wind data was analyzed for featuring wind characteristics. The measurement heights were 40, 60, and 80 m a.g.l. The LiDAR measurement campaign was carried out for one year from April 1st, 2017 to March 31st, 2018. The WindCube v2 is a pulsed Doppler laser type and the Flow Complexity Recognition (FCR) module is not installed in the system.

Table 1. Site and measurement conditions with LiDAR specification.

Items	Category		Description
Site condition	Location	Latitude	33.950287 N
		Longitude	126.309898 E
	Roughness class		1.28
Measurement condition	Measurement period	Start	1st Apr. 2017
		End	31st Mar. 2018
	Duration		12 months
	Measurement heights		40, 60, and 80 m a.g.l.
	Sampling interval		1 second
LiDAR Spec.	Model		WindCube v2
	Measuring range	Speed	0 ~ 55 m/s
		Direction	0 ~ 360°
	Accuracy	Speed	0.1 m/s
		Direction	2 °
	Operation temperature		-30 ~ +45 °C
	Type		Pulsed Doppler Laser
	Flow Complexity Recognition (FCR) module		Not installed

3. LiDAR Measurements Analysis

3.1. LiDAR wind data validation

The validation of the LiDAR data was performed before the analysis. The criteria of the LiDAR data rejection are as follows [13-15]:

- Data with Carrier-to-Noise Ratio (CNR) less than -22 dB
- Data less than 80 % availability
- Data affected by the tower's shadow

The LiDAR measurements that met the criteria above were discarded and the other measurements were used for the analysis.

Table 2 presents the recovery rate and meteorological information after the data rejection. The data recovery rate was 93.6 %, which was over the standard for acceptable rate.

Table 2. Results of data rejection.

Items	Description
Data points before and after the rejection [-]	Before 52,560 After 49,222
Recovery rate [%]	93.6
Mean temperature [°C]	15
Mean relative humidity [%]	84
Mean air density [kg/m^3]	1.21

3.2. Wind characteristics

The annual mean wind speeds were calculated at all measurement heights using the LiDAR data after the data rejection. Those were 7.42, 7.90, and 8.17 m/s at 40, 60, and 80 m a.g.l.

The Weibull wind speed distribution at 80 m a.g.l. was estimated on the basis of the actual data as a representative, which is shown in Fig. 2. The Weibull parameters of shape, k, and scale, c, were calculated by the Maximum Likelihood Estimation (MLE), which were 2.10 and 9.23 m/s, respectively. The Weibull distribution curve fit well to the actual wind speed data.

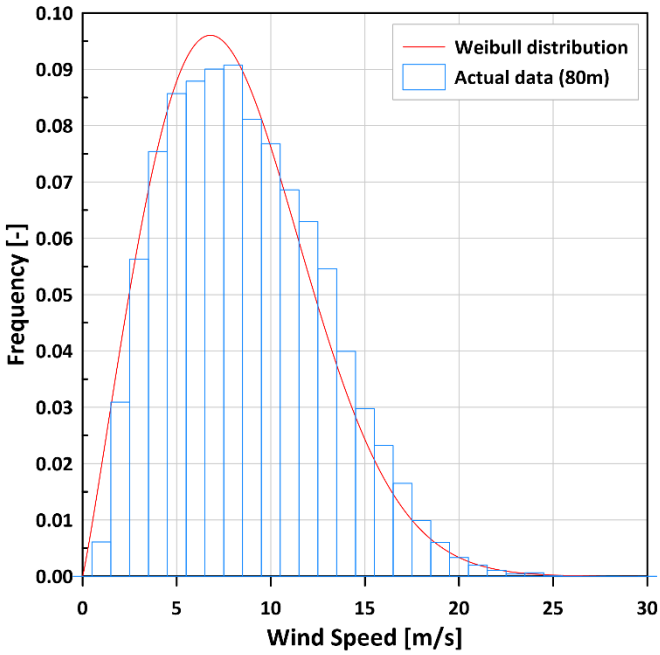

Fig. 2. Weibull distribution of wind speed at 80 m a.g.l.

Figs. 3 and 4 show the wind rose and the energy rose, respectively. The prevailing wind and energy directions were both from the NNW, which accounted for 18 % and 30 %, respectively. Directional wind frequencies were almost the same at all measurement heights, while directional energy frequencies were slightly different from one another, especially at the prevailing NNW energy direction.

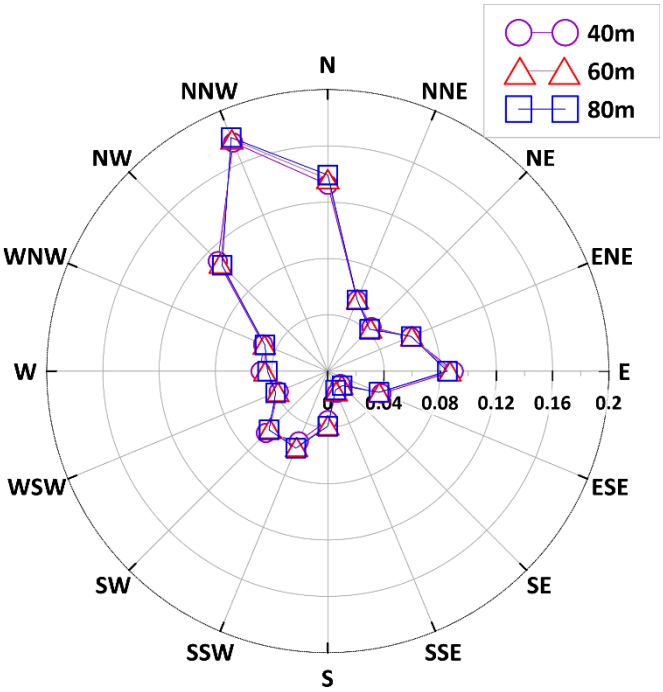

Fig. 3. Wind direction rose.

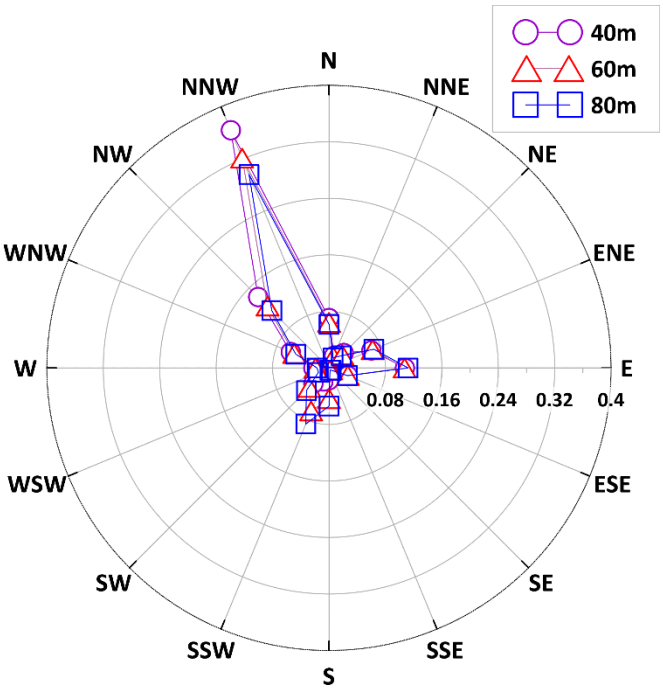

Fig. 4. Energy rose.

Fig. 5 represents the monthly mean wind speed. As the measurement height increases, the wind speed increases for all months. The highest monthly mean wind speed of 9.5 m/s was found in January, while the lowest of 6.5 m/s was in June at 80 m a.g.l. The variation in the monthly mean wind speed matched well with the normal trend of seasonal variation in Korea.

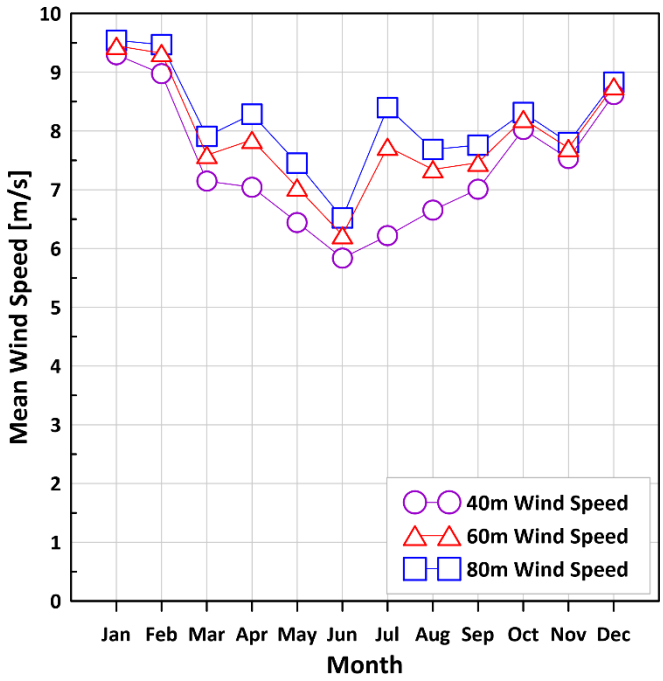

Fig. 5. Monthly mean wind speed at all measurement heights.

Fig. 6 shows the vertical wind shear. The power law is calculated by the following equation [3,4,16,17]:

$$\frac{v_2}{v_1} = \left(\frac{h_2}{h_1}\right)^{\alpha} \quad (1)$$

where, v_1 and v_2 are wind speeds at heights h_1 and h_2, respectively. α is a dimensionless power law exponent.

The power law exponent was 0.139, which corresponds to simple terrain or temperate offshore condition [3,4].

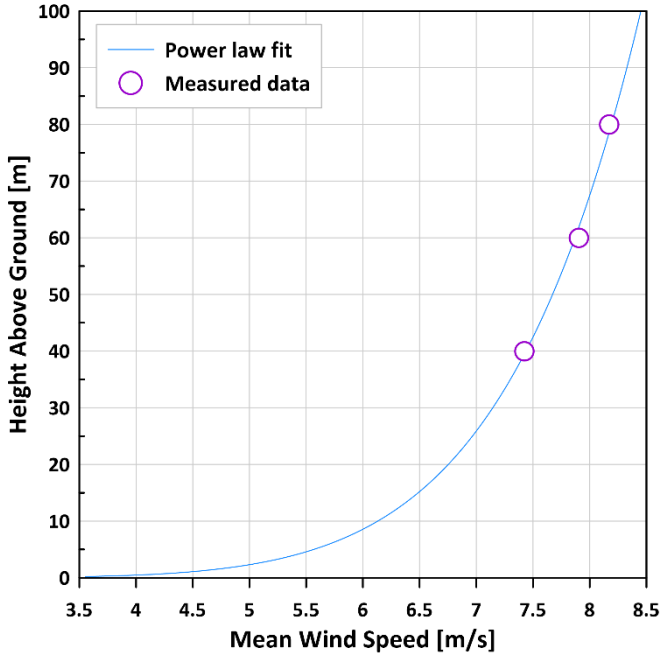

Fig. 6. Vertical wind shear.

3.3. Estimation of Annual Energy Production (AEP)

Three wind turbines from different manufacturers were chosen to analyze AEP and economic feasibility. Table 3 lists the specification of the three wind turbines. WT in the table means wind turbine. The rated power ranges from 2 MW to 3.3 MW.

Fig. 7 shows the power curves of the three wind turbines.

Table 3. Specification of wind turbines.

Items	WT A	WT B	WT C
Rated power [kW]	2,000	3,000	3,300
Hub height [m]	87	80	84
Rotor diameter [m]	86	100	112
Cut-in wind speed [m/s]	3.5	3	3
Rated wind speed [m/s]	12	13	13
Cut-out wind speed [m/s]	25	25	25

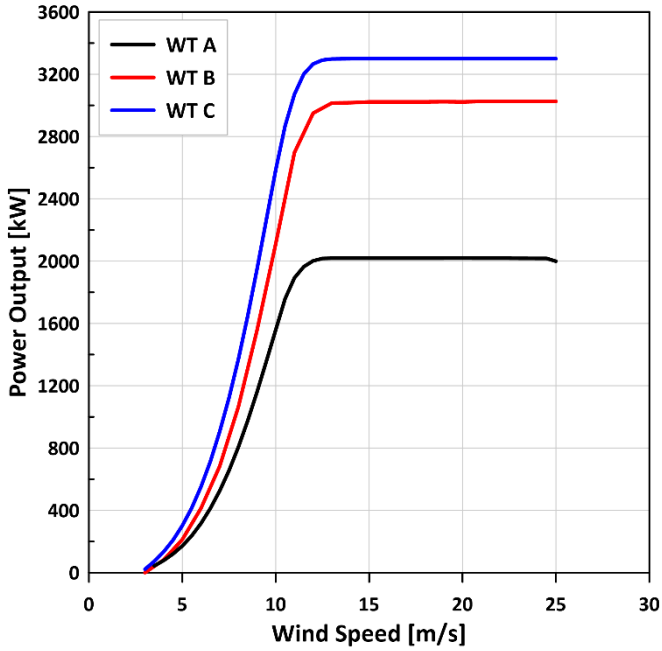

Fig. 7. Power curves of the three wind turbines.

The gross and net AEPs are calculated by the following equations [18-20]:

$$Gross\ AEP = \sum(\mathrm{p}(v_i) \times f(v_i) \times 8760) \quad (2)$$

$$Net\ AEP = Gross\ AEP - \delta \times Gross\ AEP \quad (3)$$

where, $p(v_i)$ and $f(v_i)$ are the power output and the probability density function of Weibull distribution for wind speed bin i, respectively. δ is the loss of AEP, which was assumed to be 10 % in this research.

The following equation [21,22] was used for the CF calculation:

$$CF = \frac{Net\ AEP}{Rated\ power \times 8760} \quad (4)$$

In addition, the MCP method was applied to reflect long-term wind speed. The reanalysis wind data from the Modern-Era Retrospective analysis for Research and Application, Version 2, (MERRA-2) was used for the application of the MCP method. The 25-year reanalysis wind data from 1994 to 2018 were collected at a point about 7.8 km northwest from the LiDAR measurement point. For performing the economic feasibility study, the useful life of 25 years for a wind turbine is often used in the wind industry [1,23,24]. The correlation of one-year concurrent data from LiDAR and MERRA-2 was about 0.82, which was good for conducting the MCP method [25,26]. Finally, the 25-year wind data were predicted using the Matrix method of the MCP technique, which were used for calculating annual AEPs and CFs.

The predicted annual net AEPs are shown in Fig. 8. These fluctuated from year to year for all wind turbines. As the wind turbine capacity was larger, the AEP was higher. The AEPs rapidly dropped in 2014 and remained stable since then for unknown reasons. The 25-year average AEPs were 8.29, 11.62, and 13.63 GWh for WTs A, B, and C, respectively.

Fig. 9 presents the predicted annual CFs. The same rapid drop in the CF as the AEP shown in Fig. 8 was found in 2014. The CFs of all the wind turbines were in the range of about 40 % to 50 %, which were similar to those of generic offshore wind farms. In other words, Chuja Island can be considered to have very abundant wind resources. WT A had almost the same CFs as WT C, which were all larger than those of the WT B. The average CFs over 25 years for WTs A, B, and C were 47.33 %, 44.22 %, and 47.16 %, respectively.

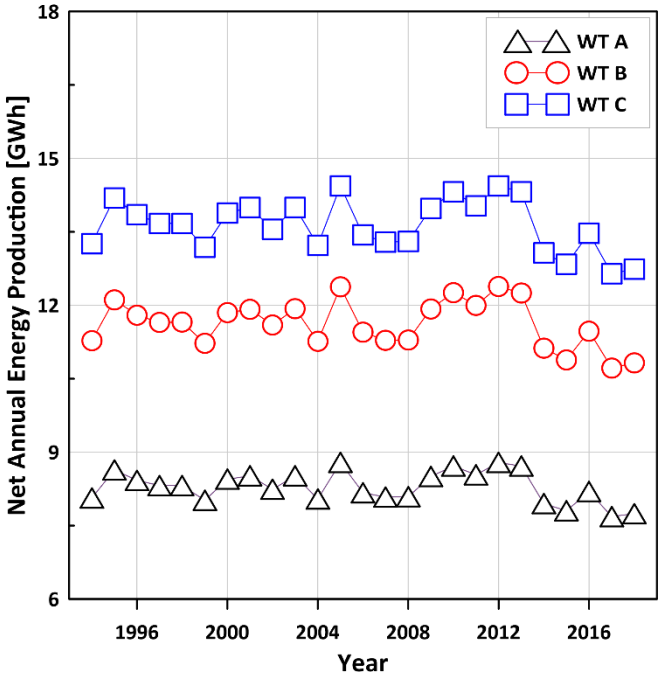

Fig. 8. Predicted annual net AEPs.

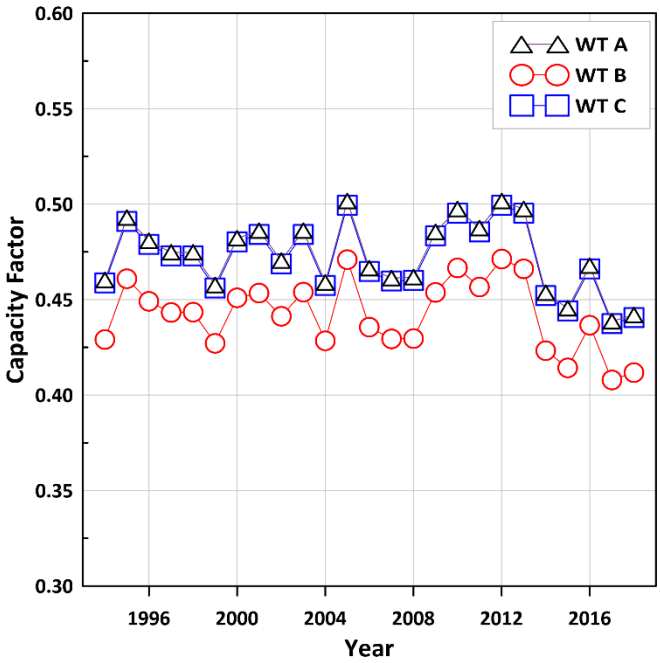

Fig. 9. Predicted annual net CFs.

4. Economic Feasibility Analysis

The economic feasibility analysis was performed using the predicted 25-year wind data. The financial assumption for the analysis is presented in Table 4. The CapEx was assumed to be 2,054.94 $/kW on the basis of an actual recent CapEx in Korea [27,28]. It was assumed that the price of a wind turbine was 0.65 of the CapEx.

The social discount rate of 4.5% in Korea was adopted as the discount rate for the analysis. The useful life of 25 years was applied. The System Marginal Price (SMP), or the electricity cost in Korea, was 0.08 $/kWh in 2017. The Operation Expenditure (OpEx) was assumed to be 3 % of the CapEx, which came from the average value of OpExs in Korea [29]. Although there is further revenue from the Renewable Energy Certificates (REC) system in Korea, it was neglected in this work.

Table 4. Financial assumption.

Items	Description
Wind turbine price* [$/kW]	1,335.71
CapEx [$/kW]	2,054.94
Discount rate [%]	4.5
Useful life [years]	25
SMP [$/kWh]	0.08
OpEx** [$/kW/yr]	61.65
*: Price of wind turbine = CapEx×0.65 **: OpEx = 0.03 × CapEx	

Four financial indicators were considered for economic feasibility analysis: Net Present Value (NPV), Benefit-Cost Ratio (BCR), Internal Rate of Return (IRR), and Simple Payback Period. Table 5 shows the results of economic feasibility analysis. As expected, the NPV became higher with an increase of the wind turbine capacity. When the NPV

values were not taken into account for the analysis, WT A had the best financial performance among the three types of WTs. Even so, WT A had very similar financial indicators of the BCR, IRR, and Payback Period to those of WT C. WT B had the worst financial performance.

Table 5. Results of economic analysis

Items	WT A	WT B	WT C
NPV [Thousand $]	4,549.96	5,792.52	7,442.46
BCR [-]	1.77	1.65	1.76
IRR [%]	13.63	12.68	13.59
Payback Period [years]	8.7	9.6	8.7

5. Year-to-year Electricity Consumption Analysis

In order to determine the possibility of energy self-sufficiency on Chuja Island, the year-to-year electricity consumption was estimated under the assumptions below:

1) The year-to-year electricity consumption has no tendency of increasing or decreasing over time.
2) The annual variability in electricity consumption follows the normal distribution based on actual electricity consumption on Chuja Island from 2014 to 2016.

The annual average electricity consumption from 2014 to 2016 on Chuja Island was 13,606,476 kWh, which was used as the mean value of the normal distribution. Then, the inter-annual variability in electricity consumption was calculated by the following equation:

$$EleCon_i = \mu(EleCon_{Chuja}) + EleCon_{var,i} \quad (5)$$

$$EleCon_{var,i} = \mu(EleCon_{Chuja}) \times \sigma_{EleCon},\ \sigma_{EleCon} \sim N(0,1) \quad (6)$$

where, $EleCon_i$ is the electricity consumption in year i. $\mu(EleCon_{Chuja})$ is the annual average electricity consumption of Chuja Island. $EleCon_{var,i}$ is the variability of electricity consumption of the island in year i. σ_{EleCon} is the standard deviation of electricity consumption.

σ_{EleCon} values of 1,000 samples were generated using a random number generator based on standard normal distribution. Then, the 25 samples corresponding to the useful life of wind turbines were extracted at random.

Fig. 10 shows the annual electricity consumption of Chuja Island estimated under the assumption above. As expected, they fluctuated around the average of 13.6 GWh. The coefficient of variation for the annual electricity consumptions was about 1 %.

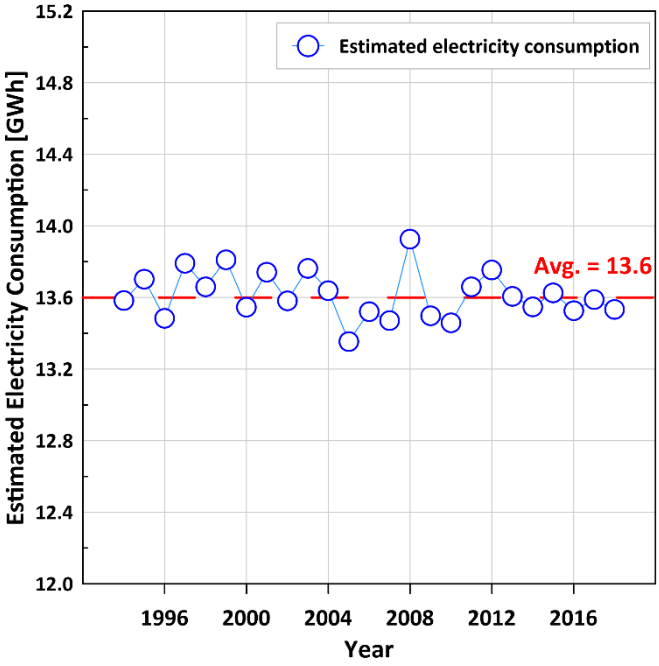

Fig. 10. Estimated electricity consumption of Chuja Island.

In order to reveal the possibility of electric energy self-sufficiency on Chuja Island, the annual ratio of the estimated net AEP to electricity consumption, which was named energy self-sufficiency ratio in this work, was calculated. Fig. 11 presents the result. The larger the wind turbine capacity was, the higher the energy self-sufficiency ratio. WT C had an average ratio of 1.0 with the range from 0.93 to 1.08, which meant that ideally, electricity demand on Chuja Island could be nearly satisfied by operating WT C by itself. An average ratio of 0.85 was calculated for WT B with the range of 0.79 ~ 0.93. The ratio for WT A was in the range of 0.57 ~ 0.66 with an average of 0.61. That is, in theory, energy self-sufficiency could be possible on Chuja Island when any two wind turbines among the studied ones are operating, which results from the abundant wind resource on Chuja Island discovered in this work.

In addition, if solar energy as well as wind energy is utilized with the Energy Storage System (ESS) for electricity generation, Chuja Island could achieve energy self-sufficiency successfully.

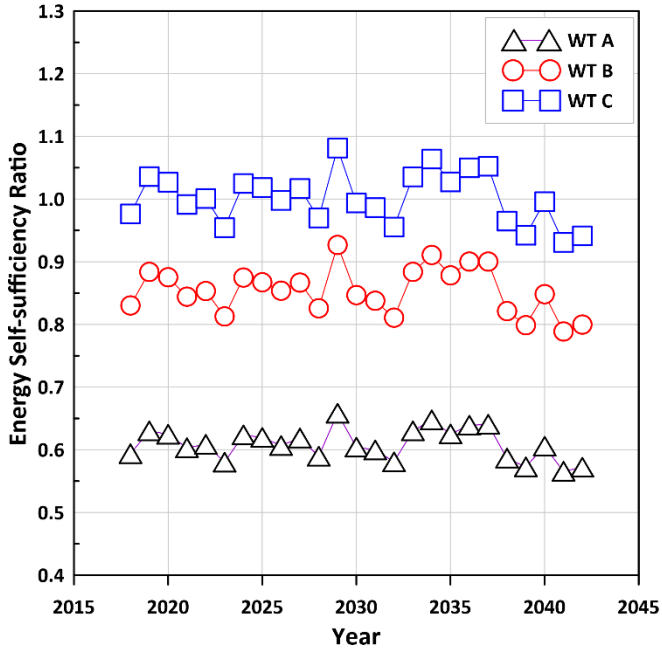

Fig. 11. Estimated annual energy self-sufficiency ratio.

6. Conclusions

The one-year wind data from the LiDAR system were used to assess the feasibility of energy self-sufficiency on Chuja Island, South Korea. The 25-year wind data were predicted using the MCP technique, which were used to estimate the 25-year AEPs of three commercial wind turbines. Then, an economic feasibility analysis was performed for the island. The results are as follows:

1) The estimated 25-year average net AEPs were more than 8.29 GWh, and the CFs were approximately 40 % to 50 %, which correspond to those of generic offshore wind farms.

2) The estimated IRRs and BCRs were at least 12.68 % and 1.65, respectively. Also, the Simple Payback Period was from 8.7 to 9.6 years. Therefore, a wind project could be economically viable at the studied site of Chuja Island in the aspect of wind energy potential.

3) As for the three wind turbines, the averages of energy self-sufficiency ratios were in the range of 0.61 to 1.0, which showed the possibility of energy self-sufficiency on Chuja Island.

Acknowledgements

This research was supported by the 2018 scientific promotion program funded by Jeju National University.

References

[1] IRENA, Renewable Power Generation Costs in 2017, International Renewable Energy Agency, 2018.

[2] IRENA, Renewable capacity statistics 2018, International Renewable Energy Agency, 2018.

[3] M. C. Brower, Wind Resource Assessment, John Wiley& Sons, Inc, 2012 pp. 105-106, 134-136.

[4] P. Jain, Wind Energy Engineering, Mc GrawHill Companies, Inc., 2011, pp. 33-35, 105-8.

[5] IEC, Wind energy generation systems Part 12-1: Power performance measurements of electricity producing wind turbines, 2nd ed., IEC 61400-12-1, International Electrotechnical Commission, 2017.

[6] D. Kim, J. Hyeon, D. Shin, B. Ju, K. Ko, and J. Huh, "Measurements and verification of ground-based LiDAR in complex terrain", In: 2015 International Conference on Renewable Energy Research and Applications [ICRERA], Palermo, IEEE, pp. 1575-1579, November 2015.

[7] J. Kim, K. Oh, M. Kim, K. Kim, "Evaluation and Characterization of offshore wind resources with long-term met mast data corrected by wind lidar", Renewable Energy, pp. 1-15, 2018.

[8] D. Choi, W. Shin, K. Ko, "Rhee Won-Jong, Static and Dynamic Yaw Misalignments of Wind Turbines and Machine Learning Based Correction Methods Using LiDAR Data", IEEE Transactions on Sustainable Energy, Vol. 10, No. 2, pp. 971-982, 2019.

[9] D. Gulli, E. Avolio, C. R. Calidonna, T. L. Feudo, and R. C. Torcasio, "Two years of wind-lidar measurements at an Italian Mediterranean Coastal Site", Energy Procedia, Vol. 125, pp. 214-220, 2017.

[10] S. Wharton, G. Qualley, J. Newman, and W. Miller, 2013 LIDAR Campaign at Buena Vista Wind Farm: An Examination of Hill Speedup Flows, Lawrence Livermore National Lab. (LLNL), Livermore, CA (United States), 2013.

[11] S. Rehman, M. A. Mohandes, L. M. Alhems, "Wind speed and power characteristics using LiDAR anemometer based measurements", Sustainable Energy Technologies and Assessments, Vol. 27, pp. 46-62, 2018.

[12] M. D. Mifsud, T. Sant, R. N. Farrugia, "A comparison of Measure-Correlate-Predict Methodologies using LiDAR as a candidate site measurement device for the Mediterranean Island of Malta", Renewable energy, Vol. 127, pp. 947-959, 2018.

[13] Leosphere, WindCube V2 LiDAR Remote Sensor User Manual version 06, Leosphere, pp. 18-9.

[14] B. Cañadillas, A. Westerhellweg, T. Neumann, Testing the Performance of a Ground-based Wind LiDAR System, DEWI Magazine, No. 38, pp. 58-64, 2011.

[15] D. Kim, T. Kim, G. Oh, J. Huh, K. Ko, "A comparison of ground=based LiDAR and met mast wind measurements for wind resource assessment over various terrain conditions", Journal of Wind Engineering and Industrial Aerodynamics, Vol. 158, pp. 109-121, 2016.

[16] S. Akdağ, Ö. Güler, E. Yağci, "Wind speed extrapolation methods and their effect on energy generation estimation", In: 2013 International Conference on

Renewable Energy Research and Applications [ICRERA], IEEE, pp. 428-430, October 2013.

[17] S. Ozcira, N. Bekiroglu, A. Agcal, "A study on feasibility of wind energy production in Silivri region by using laboratory setup", In: 2013 International Conference on Renewable Energy Research and Applications [ICRERA], IEEE, pp. 1175-1179, October 2013.

[18] K. Ko, J. Huh, The introduction to wind engineering, Seoul: MoonUnDang, 2006, ch. 4.

[19] A. Hossieni, V. Rasouli, S. Rasouli, "Wind energy potential assessment in order to produce electrical energy for case study in Divandareh, Iran", In: 2014 International Conference on Renewable Energy Research and Application [ICRERA], IEEE, pp. 133-137, October 2014.

[20] F. Wendt, K. Lo, S. Wang, "Influence of wind conditions on siting, design and performance considerations for offshore wind turbines in the Gulf of Mexico region", In: 2012 International Conference on Renewable Energy Research and Applications [ICRERA], IEEE, pp. 1-6, November 2012.

[21] B. Ju, J. Jeong, K. Ko, "Assessment of Wind Atlas Analysis and Application Program and computational fluid dynamics estimates for power production on a Jeju Island wind farm", Wind Engineering, Vol. 40, No. 1, pp. 59-68, 2016.

[22] G. Gualtieri, "Development and application of an integrated wind resource assessment tool for wind farm planning", International Journal of Renewable Energy Research [IJRER], Vol. 2, No. 4, pp. 674-685, 2012.

[23] S. Tyler, H. Donna, S. George, 2017 cost of wind energy review, No. NREL/TP-6A20-72167, National Renewable Energy Lab. [NREL], Golden, CO [United States], 2018.

[24] International Energy Agency, Nuclear Energy Agency, Projected Costs of Generating Electricity-2015 Edition, Ogranisation for Economic Co-operation and Development, Paris, France, 2015.

[25] EMD International Corp., WindPRO 2.9 User Guide, EMD International Corp., pp. 601-633, 2013.

[26] D. Todorović, Ž. Đurišić, J. Tuševljak, "A day-ahead real net transfer capacity forecast based on the prediction of the real cooling conditions for interconnection overhead lines", In: 2015 International Conference on Renewable Energy Research and Applications [ICRERA], IEEE, pp. 630-635, November 2015.

[27] K. Lee, K. Ko, "Analysis of LCOE for Korean Onshore Wind Farms using Monte Carlo Simulation", The 2018 Fall Conference of Korea Wind Energy Association, Busan, Korea, pp. 27-30, October 2018.

[28] Korea Energy Economics Institute, Study on Estimation of Levelized Cost of Energy by a power source, Korea Power Exchange [KPX], Korea, 2018.

[29] C. Min, D. Hur, J. Park, "Economic Evaluation of Offshore Wind Farm in Korea", The Transactions of the Koeran Institute of Electrical Engineers, Vol. 63, No. 9, pp. 1192-1198, 2014.